

Communication

Discrete Au₁(0) Stabilized by 15-Crown-5 for High-Efficiency Catalytic Reduction of Nitrophenol and Nitroaniline

Xing Shen^{1,2} and Kairui Liu^{1,*}

¹ State Key Laboratory of Catalysis, Dalian National Laboratory for Clean Energy, Dalian Institute of Chemical Physics, Chinese Academy of Sciences, 457 Zhongshan Road, Dalian 116023, China

² University of Chinese Academy of Sciences, Beijing 100049, China

* Correspondence: liukairui@163.com

Abstract: Single-atom catalysts (SACs) have been synthesized using a variety of methods in recent years, and they have shown excellent catalytic activities. However, metal atoms show a high tendency to agglomerate in liquid media, making the single atom synthesis more difficult in liquid media. The synthesis of such metal single-atom catalysts that do not have strong ligand coordination is rarely reported in the literature. Herein, we report the facile synthesis of monodispersed Au atoms (Au₁) through the reduction in HAuCl₄ in 15-crown-5. The complete reduction in HAuCl₄ was confirmed through UV-Vis spectroscopy. In addition, the Au was found in a zero valence state after reduction, which was confirmed through XPS and XANES results. Moreover, the dispersion of Au was confirmed as a single atom (Au₁) through transmission electron microscopy and spherical aberration electron microscopy. The possible structure of this catalyst was proposed by matching the EXAFS results with the structure of Au₁@15-crown-5 as -(OC₂H₄O)-AuCl₂H₂. The Au₁@15-crown-5 showed high activity (TOF as high as 22,075) in the reduction in nitrophenol and nitroaniline to aminophenol and phenylenediamine by sodium borohydride. Because of the monodispersion of Au atoms, its performance is much better than noble nanoparticles and non-precious metal catalysts.

Keywords: gold; single atom; nitroaromatic compounds reduction; catalysis



Citation: Shen, X.; Liu, K. Discrete Au₁(0) Stabilized by 15-Crown-5 for High-Efficiency Catalytic Reduction of Nitrophenol and Nitroaniline. *Catalysts* **2023**, *13*, 776. <https://doi.org/10.3390/catal13040776>

Academic Editors: Leiduan Hao and Jilei Xu

Received: 14 March 2023

Revised: 12 April 2023

Accepted: 14 April 2023

Published: 20 April 2023



Copyright: © 2023 by the authors. Licensee MDPI, Basel, Switzerland. This article is an open access article distributed under the terms and conditions of the Creative Commons Attribution (CC BY) license (<https://creativecommons.org/licenses/by/4.0/>).

1. Introduction

Au is one of the earliest noble metals recognized and utilized by human beings. Au catalysts have unique catalytic properties due to their higher Lewis acidity and electronegativity caused by relativistic effects and low coordination index crystal surfaces [1,2]. However, it has limited use in the catalysis industry due to its poor dispersibility and the perception that it is chemically inert and expensive [3]. The German company Knapsack discovered the first heterogeneous catalyst containing gold, which was used for the oxidative acetoxylation of ethylene to vinyl acetate [4]. Since then, gold catalysts have been developed for various reactions, and they have shown excellent performance in various reactions, such as CO low-temperature oxidation, ethyl hydrochlorination, selective hydrogenation of butanaldehyde, water gas conversion, and NO_x reduction. Additionally, research on gold catalysts for the oxidation of olefins, alcohols, and even alkanes is progressing rapidly. Zhang Tao and colleagues employed a straightforward adsorption impregnation technique with chloroauric acid as the precursor to create a range of carrier-loaded gold single-atom catalysts, including iron oxide, cobalt oxide, and cerium oxide. These catalysts were then tested for their efficacy in CO oxidation reactions, and the findings revealed that all of the single-atom catalysts exhibited equivalent turnover frequencies (TOF) and higher reaction rates than 2–3 nm nano-Au [5]. Avelino Corma discovered that the selective reduction in aliphatic nitro compounds, paired with aldehydes in hydrogen, on gold catalysts resulted in a significant increase in the selectivity of nitro reduction catalyzed by Au/TiO₂, increasing from 50% to 90%, as compared to Pt catalysts loaded with carbon [6]. Yong Cao employed

loaded gold nanocatalysts for the selective reduction in furfural in aqueous phase media, substituting H_2 with a low-cost, abundant CO source, to achieve a highly specific catalytic conversion of furfural to furfuryl alcohol [7]. Gold catalysts are also replacing expensive precious metal catalysts, such as Pd and Rh, in many industrial processes, which is significant for both scientific research and industrial production.

Single atoms catalysts (SACs), as a term, was first proposed in 2011 in a seminal work by Prof Zhang and coworkers [8]. This concept has been gradually accepted by the catalysis field as one of the most innovative and active research frontiers. For example, take the noble metal catalysts: when the catalyst particle dispersion reached the monatomic scale, the dramatically increased surface free energy, the quantum size effect, the interaction of the unsaturated coordination environment, and the catalyst-support correlation had many advantages such as ultra-high activity and selectivity, nearly 100% atom-utilization efficiency, the easy identification of reaction mechanisms, lower cost, etc. [9]. SACs have been extensively explored for various applications, including oxygen reduction reactions, carbon dioxide reduction, nitrogen reduction, organic synthesis, and storage applications [10]. Due to their high free energy, they are easy to agglomerate to clusters/nanoparticles during preparation and reaction, resulting in catalyst deactivation. The preparation method of SACs with high stability and load capacity is an important topic.

To tackle such problems, a valid approach is to employ strong carrier–metal interactions in the preparation of SACs [11,12]. However, there are few reports about the preparation of zero-valent mononuclear metal atoms that exist stably in solution. Metal atoms monodispersed in solution can be supported by exploiting their weak interaction with inert support, including crown ethers and other polymers. Moreover, it is more convenient to build a stable multinuclear controllable system in a solution than to use other methods that rely on a strong interaction between the support and the metal. The synthesis of Pt single-atom catalysts that exist stably in solutions has been reported using PDMS-PEG, 15-crown-5, and EGDE; however, the synthesis of Au single-atom catalysts is rarely reported [13–15]. Crown ethers have been widely used for the capture and complexation of different metal ions. In addition, 15-crown-5 has been used as a protective agent previously to successfully synthesize Pt single-atom catalysts that exist stably in solution.

Nitrophenol and nitroaniline are nitroaromatic toxic intermediates released in large quantities from various medical sectors and pesticide industries. Nitroaromatic compounds are regarded as generally toxic, carcinogenic, mutagenic, etc., because of the existence of the reactive nitro group [16]. 4-nitrophenol and 2-nitroaniline have been listed as priority pollutants by the U.S. Environmental Protection Agency because they are either precursors or derivatives of a vast number of pollutants [17]. The removal of nitroaromatic compounds from solution is carried out through various conventional methods, including the electro-Fenton method [18], the photocatalytic degradation [19], the electrochemical method [20], and the chemical catalytic reduction method [21]. Compared with other technologies, the catalytic reduction in nitroaromatic compounds has proven to be more effective due to its low energy consumption and relatively clean process. Compared with traditional non-noble metal-based catalysts, noble metal-based catalysts often have higher catalytic performance [22].

Herein, we report the synthesis of a zero-valent mononuclear Au single-atom catalyst that stably exists in the solution using 15-crown-5 as the protective agent. The catalyst was then applied to the reduction in nitroaromatic by sodium borohydride and showed extremely high reactivity.

2. Result and Discussion

The synthesis of $Au_1@15\text{-crown-5}$ was characterized by UV-visible spectroscopy. The UV-Vis absorption peak of $[AuCl_4]^-$ at 323 nm disappeared with time [23], indicating $HAuCl_4$ is completely reduced. At the same time, the absorption peak of $[AuCl_2]^-$ was at 240 nm, and no obvious peak of 240 nm was observed from Figure 1, so there was no accumulation of $[AuCl_2]^-$ during the reaction [24]. The characteristic broad peaks of Au

nanoparticles were not observed between 400 and 600 nm [23], revealing that there were no Au nanoparticles in the system (as shown in Figure 1). In addition, the color of the solution changed from yellow to colorless after reduction, also indicating the reduction in the HAuCl_4 .

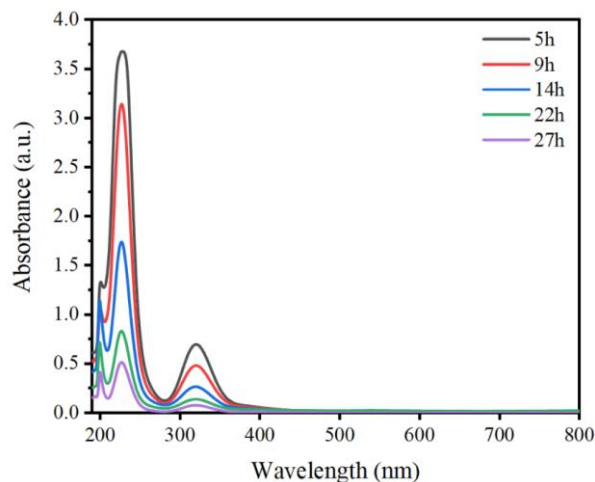


Figure 1. UV-visible spectra of the reduction in HAuCl_4 at different time intervals.

To further confirm the oxidation state of Au_1 , the XPS analysis of the solid ($\text{Au}_1@15\text{-crown-5}/\text{TiO}_2$) sample was performed. It was observed (Figure 2) that the characteristic absorption peaks of the electronic binding energy of the $\text{Au}@15\text{-crown-5}$ appeared at 87.1 eV ($4f_{5/2}$) and 83.4 eV ($4f_{7/2}$); these were very close to the zero-valent standard gold sample (i.e., 87.43 eV, 83.74 eV) [25]. This result confirmed that the gold atoms in $\text{Au}@15\text{-crown-5}$ were completely reduced.

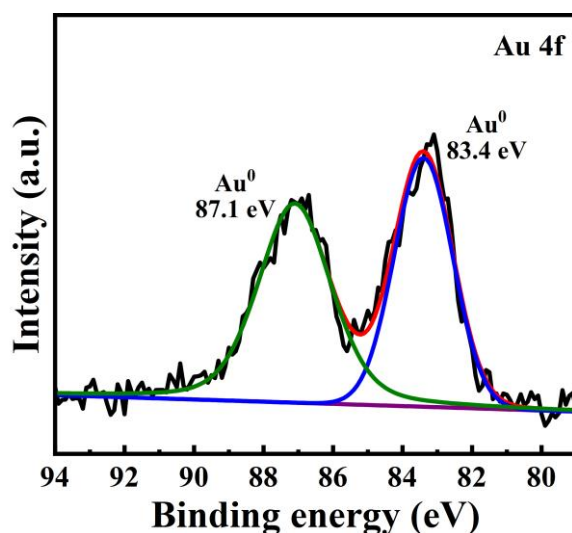


Figure 2. X-ray photoelectron spectra (XPS) of the synthesized $\text{Au}@15\text{-crown-5}$ catalyst.

The dispersion of Au atoms in $\text{Au}_1@15\text{-crown-5}$ supported by the oxide support (TiO_2) was studied by transmission electron microscopy and spherical aberration electron microscopic techniques. The transmission electron microscopy results of 0.5 wt.% $\text{Au}@15\text{-crown-5}/\text{TiO}_2$ (Figure 3a,b) confirmed that there were no Au clusters. Moreover, the HAADF-STEM image shows that only mononuclear Au atoms are uniformly dispersed on the TiO_2 surface (Figure 3c,d). Therefore, it is inferred that the dispersion of Au atoms in the $\text{Au}_1/15\text{-crown-5}/\text{ethanol}/\text{H}_2\text{O}$ solution is single-atom.

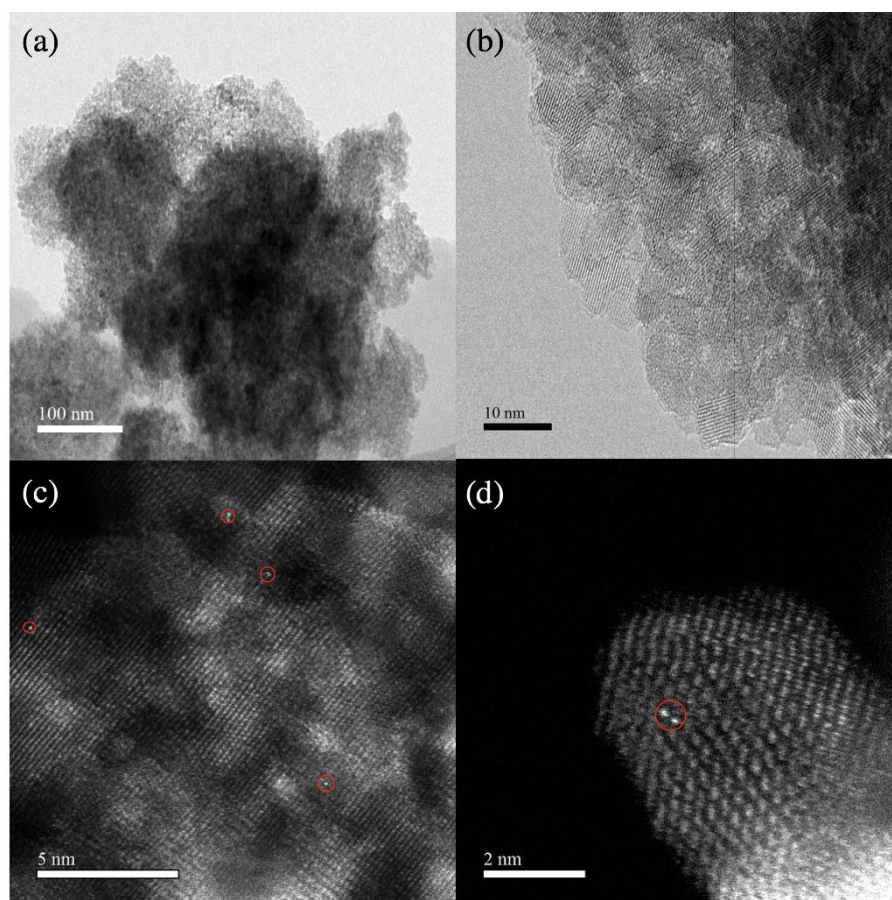


Figure 3. TEM and spherical aberration electron microscopic images of Au₁@15-crown-5 at different magnifications: (a,b) TEM images; (c,d) HAADF-STEM images.

To confirm the composition of the catalyst, EDX analysis was performed, and it confirmed the presence of the Au element. The results showed that the mass fraction of Au was 0.76 wt.% (Figure S1), the theoretical Au content of the sample was 0.5 wt.%, and the error was within the allowable range.

To gain more information on the electronic and coordination structures of the Au₁ atoms in Au₁@15-crown-5, X-ray absorption spectroscopy (XAS) was carried out. The XANES spectrum of the synthesized Au₁@15-crown-5 loaded on SiO₂ and Au foil (used as reference material) is shown in Figure 4a. As we know, XANES is very sensitive to the valence state, and the higher the absorption edge moves to the higher energy, the higher the valence state. The edge absorption energy in the XANES spectrum of SAC is similar to that of the reference Au foil, indicating that Au(0) is the main Au species present in Au₁@15-crown-5, which is also consistent with the XPS results above.

After that, the EXAFS data are processed and converted into wavelength-k-space oscillations. The data in R-space can be obtained by Fourier transform in K-space, and the data in the Q-space can be obtained by inverse Fourier transform in R-space. By comparing the peak patterns of the K space and Q space spectra, if the peak patterns are similar, it can be confirmed that the range of K space selected by Fourier transform to R space is reasonable (Figure S2).

In the R-space diagram (Figure 4b), there is an obvious peak at about 1.9 Å for the Au₁@15-crown-5, which is different from that of the Au-Au bond in the Au foil at 2.6 Å. The absence of peak at 2.6 Å indicates that there are no Au clusters/nanoparticles in the sample. This is also consistent with the electron microscope results above.

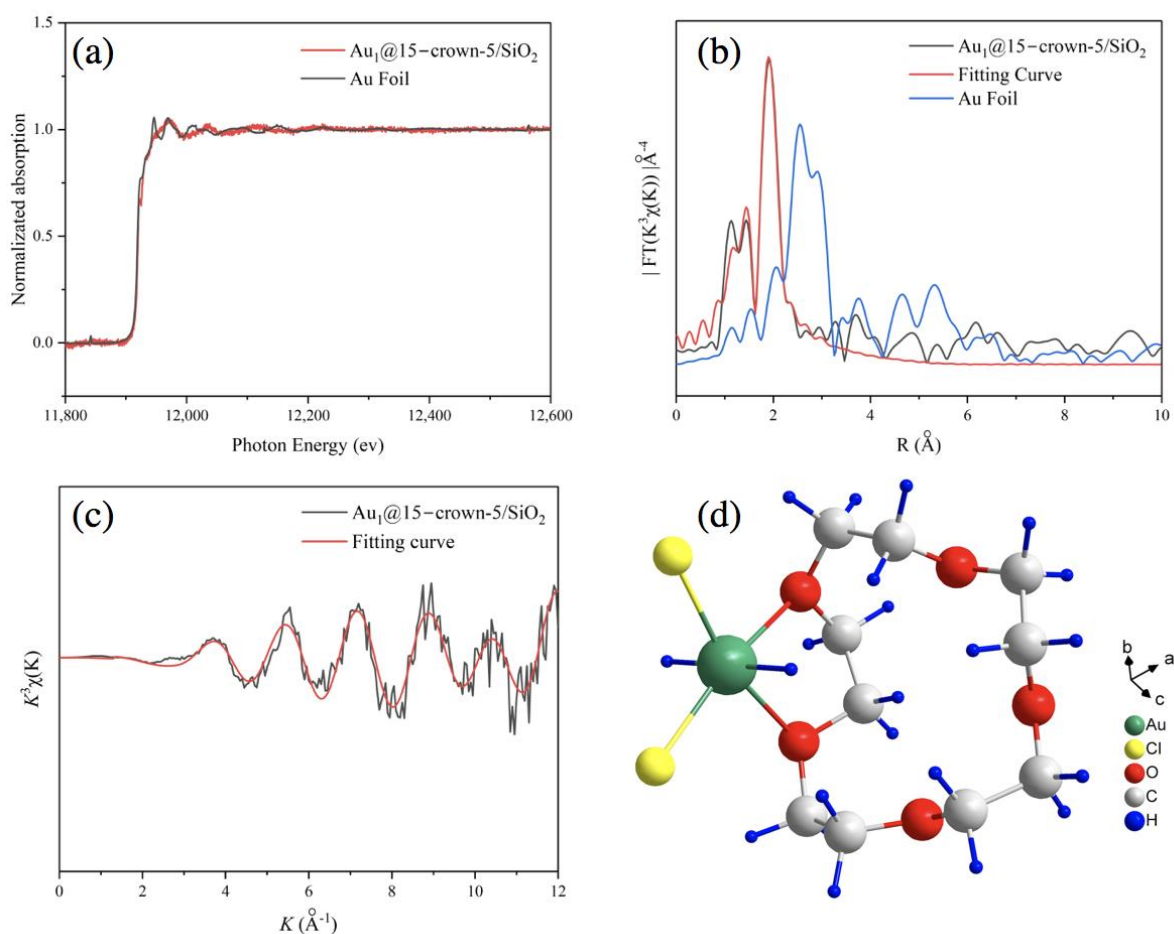


Figure 4. X-ray absorption spectroscopy analysis (XAS) of Au₁@15-crown-5: (a) E-Space of Au₁@15-crown-5/SiO₂ and Au foils; (b) R-space of Au₁@15-crown-5/SiO₂, Au foil and fitting curve; (c) K-Space of Au₁@15-crown-5/SiO₂ and fitting curve; and (d) structure mode of Au@15-crown-5.

According to the synthesis process of our catalyst, the system contains ethanol, water, hydrogen chloride, and 15-crown-5. We consider that the elements that may coordinate with Au include H, O, and Cl. The XPS-Cl_{2p} spectrum shows that some Cl ions may still be weakly coordinated to Au₁ (Figure S2). In addition, if 15-crown-5 is not added to the system, Au₁ cannot be synthesized, so it is likely that Au₁ is also coordinated by O of 15-crown-5. In addition, according to the results of XPS and XENES, Au shows a zero-valence state, so there may also be a certain H coordination to neutralize the positive charge of Au. So, we refer to the bond length of the Au-O bond and Au-Cl bond in Au₂O₃ and AuCl₃ crystal cells as the initial value of EXAFS fitting. The fitting data results are shown in Table S1, and the R-space and K-space spectra after fitting compared with the experimental data are shown in Figure 4b,c. The fitting results and the experimental results match well in the R-space and K-space spectra. Meanwhile, a schematic model of the Au₁ coordination environment in the Au₁@15-crown-5 was given in Figure 4d, and the calculated bond length was consistent with the EXAFS fitting results.

The synthesis procedures of Au₁@15-crown-5 are shown in Figure 5. It reveals that one [AuCl₄]²⁻ is reduced to [AuCl₂]⁻ by ethanol, and ethanol is oxidized to acetaldehyde. The protons in ethanol combine with Cl atoms to form HCl. The reduction [AuCl₂]⁻ is similar to that of [AuCl₄]⁻. Finally, crown ether and H⁺ coordinate with Au to form a stable-present monatomic structure in solution.

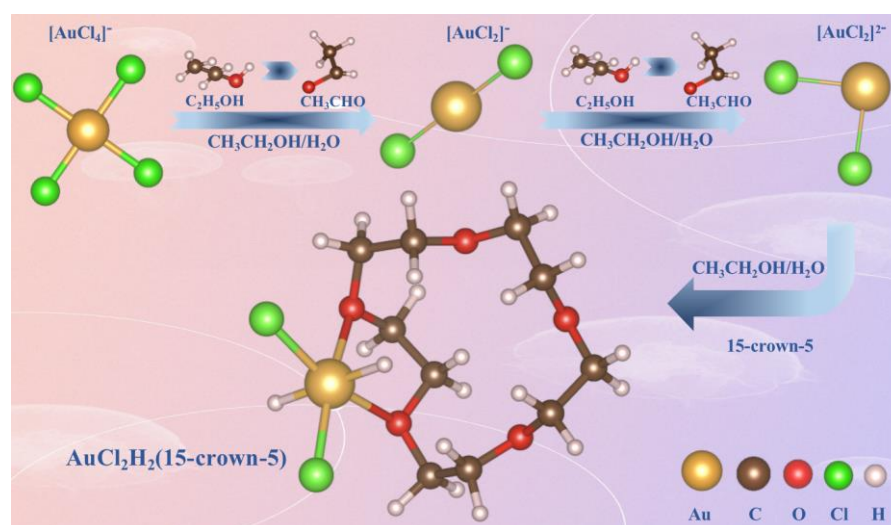


Figure 5. Synthesis procedures of $\text{Au}_1@15\text{-crown-5}$.

The catalytic reduction is one of the most important applications of Au. The catalytic activity of the $\text{Au}_1@15\text{-crown-5}$ catalyst was tested by reducing the toxic 4-nitrophenol (4-NP) to less toxic 4-aminophenol (4-AP), which is one of the benchmark reactions in contaminant degradation. Due to the formation of 4-nitrophenolate ion in an alkaline environment, the absorption peak of 4-NP was red-shifted to 400 nm, and the color of the solution ranged from light yellow to yellow-green. Without the addition of $\text{Au}@15\text{-crown-5}$ catalyst, the mixture of 4-NP and NaBH_4 retained the color of the solution and the intensity of the UV absorption peak at 400 nm unchanged for an extended period (i.e., 600 min), as shown in Figure 6a, indicating that NaBH_4 cannot reduce 4-nitrophenol by itself. However, after adding $\text{Au}_1@15\text{-crown-5}$ catalyst, the color of the mixture changed from yellow-green to colorless in about 30 min at room temperature, indicating that the $\text{Au}_1@15\text{-crown-5}$ catalyst prepared in this work can efficiently catalyze the reduction in 4-NP. The calculation shows that the TOF value is as high as $22,075 \text{ h}^{-1}$, which is 5 times higher than the non-noble metal complexes catalyst ($\text{eHA}@\alpha\text{-Ni(OH)}_2$) [26] and more than 2 times higher than the noble metal catalyst (Au/MOF) [27] (Figure 6d); compared to the Au nanoparticle catalysts (Au NPs-graphene oxide nanosheets), we have greatly reduced the amount of Au (about 50 times) for the same reaction time and correspondingly increased TOF by more than 50 times [28]. In addition, the TON is 11,038 with almost 100% conversion (Figure 6b). If we increase the quantity of the catalyst, the reaction time can be reduced to less than 4 min (Figure S4).

The reduction in 4-NP by NaBH_4 has been widely used as a model reduction reaction since it is easy to monitor with simple and fast analytical techniques, and there are no by-products. This reaction is also valuable in the view of green chemistry since 4-NP, one of the toxic substances in the wastewater, is converted into a commercially important substance, 4-AP [23]. In a previous study, in addition to the etched Halloysite nanotubes mentioned above (the $@\alpha\text{-Ni(OH)}_2$ catalyst and the Au/MOF catalyst), non-noble metals such as Cu, Fe, and Co, noble metals such as Pt, Pd, and Ag are also designed as 4-NP reduction catalysts. We summarized this in Table S2. The synthesized catalyst in our study is mild and more efficient than the previous reported ones.

Further reducing the amount of Au mono-atoms to $0.2 \mu\text{L}$ (150 mL 4-NP), the TON value can reach as high as 205,298. However, deactivation occurred in such situations, as is shown in Figure 6c. The deactivation of the catalyst may result from the aggregation of Au_1 species into clusters/nanoparticles, as is shown in Figure S5.

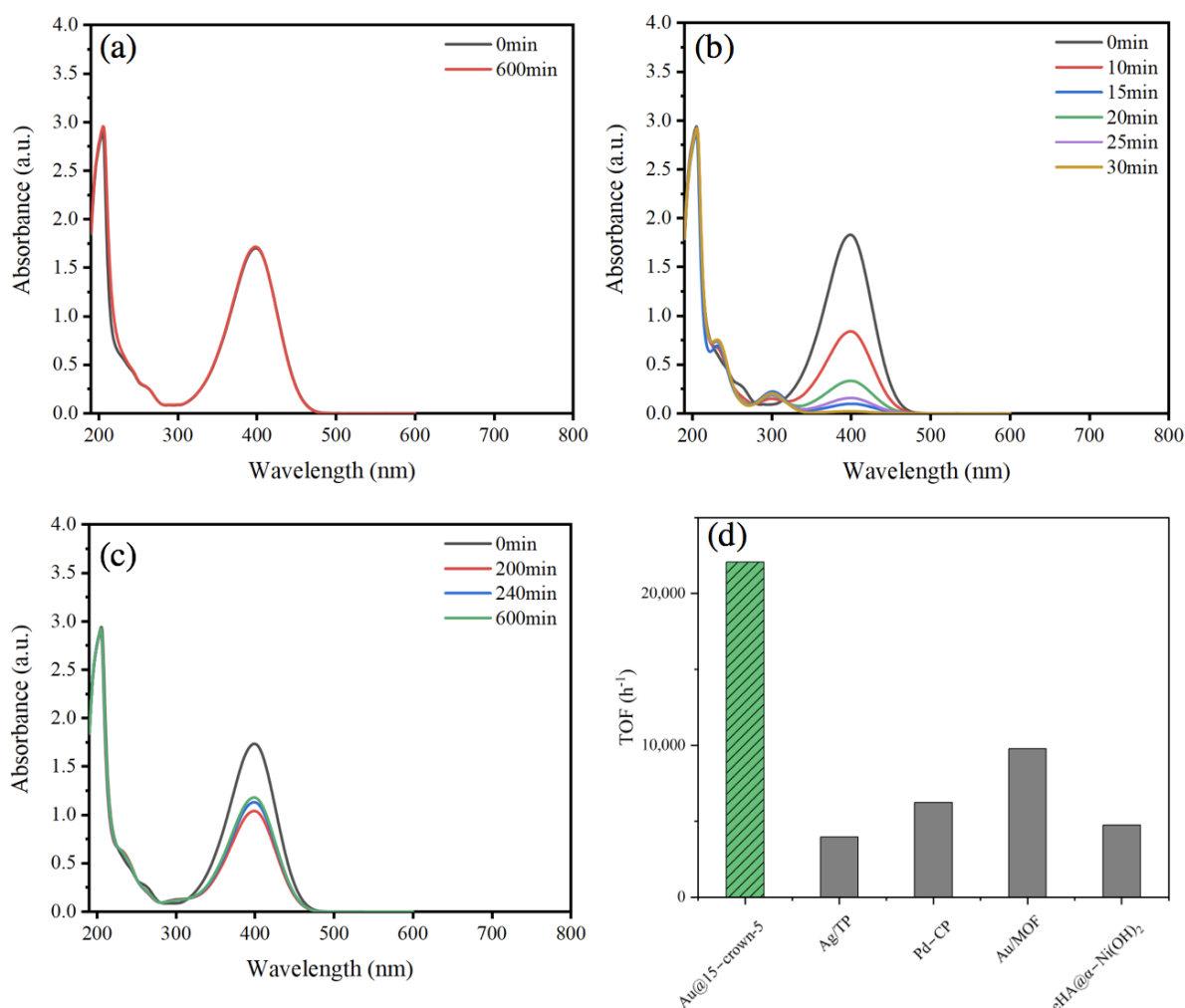


Figure 6. Catalytic reaction properties of Au@15-crown-5: (a), NaBH₄ + 4-NP; (b), NaBH₄ + 4-NP + Au@15-crown-5 catalyst at different time intervals up to 30 min; (c), NaBH₄ + 4-NP + Au@15-crown-5 catalyst at different time intervals up to 600 min; and (d) comparison of catalytic performance of other catalysts and this work.

We also used the Au₁@15-crown-5 to determine the catalytic reduction in 2-NP, 2-NA, and 4-NA(nitroaniline) according to the abovementioned outcomes. The reduction in these compounds can also be easily monitored by UV-Vis. As is shown in Figure 7, Au₁@15-crown-5 also has high activity for the reduction in other nitroaromatics. The results suggest that these compounds can be effectively reduced, and the catalytic rate follows the order of 4-NP > 2-NP > 2-NA > 4-NA with TOF of 22,075, 13,245, 11,038, and 10,348 h⁻¹, respectively (the calculation of TOF is described in the supporting information), demonstrating the universality of this catalyst in the reduction in nitrophenol and nitroaniline.

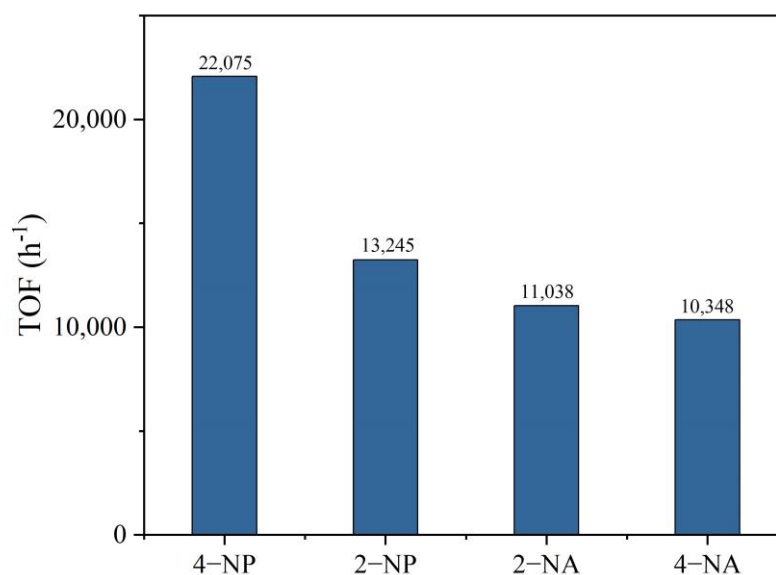


Figure 7. Reactivity of other nitroaromatic by single-atom catalysts.

3. Materials and Methods

3.1. Materials

All of the chemicals used in this work, i.e., $\text{HAuCl}_4 \cdot \text{H}_2\text{O}$ (AR) and absolute ethanol (AR), were purchased from Sinopharm Chemical Reagent Co., Ltd., Shanghai, China; 15-crown-5 (AR) was purchased from Tokyo Chemical Industry (TCI), Tokyo, Japan; TiO_2 (AR), SiO_2 (AR), 4-nitrophenol (AR), 4-nitroaniline (AR), 2-nitrophenol (AR), and 2-nitroaniline (AR) were purchased from Shanghai Aladdin Bio-Chem Technology Co., Ltd., Shanghai, China; and NaBH_3 (AR) was purchased from Tianjin Damao Chemical Reagent Co., Ltd., Tianjin, China. The chemicals were directly used without any further treatment.

3.2. Synthesis of Catalyst

The catalyst ($\text{Au}_1@15\text{-Crown-5}$) was prepared by stirring 15-Crown-5 (0.8 g) in ethanol (270 mL) and water (27.2 mL) mixture for 30 min at room temperature to make 15-Crown-5 uniformly dispersed. After 30 min, 2.8 mL of the HAuCl_4 aqueous solution (24.3 mM) was added to the 15-Crown-5 solution and stirred further for 10 min at room temperature. Then, the temperature was slowly increased to 65 °C, the mixture was stirred for 27 h, and then the mixture was cooled to room temperature gradually.

$\text{Au}_1@15\text{-crown-5}/\text{TiO}_2$ was prepared for the analysis by taking the $\text{Au}_1@15\text{-crown-5}$ (40 mL) solution and nano- TiO_2 (0.35 g) together and stirred in a round bottom flask for 1 h. After that, the solvent was removed under reduced pressure at 40 °C and placed in a vacuum oven at 40 °C for further drying for 12 h.

3.3. UV-Vis Absorption Spectroscopy

UV-Vis (Shimadzu UV-2600, Tokyo, Japan) was used to monitor the reduction process of HAuCl_4 . An appropriate volume of the reaction solution was added to the UV cuvette at different time intervals and read spectroscopically from 190–800 nm each time. The absorption peak of $[\text{AuCl}_4]^-$ was monitored at 323 nm.

3.4. X-ray Photoelectron Spectroscopy (XPS) Analysis

X-ray photoelectron spectroscopy (XPS) analysis was carried out to get the oxidation chemical state information of $\text{Au}_1@15\text{-Crown-5}$. $\text{Au}_1@15\text{-crown-5}/\text{TiO}_2$ was used as a test sample, and the preparation method is described in 3.2.

XPS experiment was carried out on X-ray photoelectron spectrometer (Thermo ESCALAB 250Xi, Waltham, MA USA) using monochromatic $\text{Al K}\alpha$ (1486.6 eV, 15 kV, and

10.8 Ma) as an excitation source. The sample was pressed in the glove box and then fixed on the sample holder with special ultra-high vacuum insulation tape. The sample was then put into a rapid sample chamber and sample preparation chamber and evacuated step by step and placed in the analysis chamber for measurement. The analysis was carried out keeping 1×10^{-8} Pa background pressure and 7.1×10^{-5} Pa working pressure. Energy resolution was kept as 20 eV, FWHM ($\text{Ag}_{3d_{5/2}}$) = 0.65 eV (metal counterfeit standard sample).

3.5. Transmission Electron Microscopic Analysis (TEM)

The transmission electron microscope (JEOL JEM-2000EX, Tokyo, Japan) with 120 kV accelerating voltage was used to check whether there are Au nanoparticles in the fresh catalyst or not. The sample ($\text{Au}_1@15\text{-crown-5/TiO}_2$) was prepared in the same way as described for XPS analysis.

3.6. Spherical Aberration Electron Microscopic Analysis

A spherical aberration electron microscope (JEOL JEM-ARM200F, Tokyo, Japan) was used to check whether the dispersion of Au was single atoms or not. The sample ($\text{Au}_1@15\text{-crown-5/TiO}_2$) was prepared in the same way as described for XPS analysis.

3.7. X-ray Absorption Spectroscopy (XAS) Analysis

The X-ray absorption spectroscopy (Advanced Photon Source, Lemont, IL USA) technique was used to determine the local geometric and/or electronic structure of the product. The sample ($\text{Au}_1@15\text{-crown-5/SiO}_2$) was prepared in the same way as described for XPS analysis, except that the catalyst support was replaced with SiO_2 .

3.8. Catalytic Efficiency Evaluation

To check the catalytic efficiency of synthesized $\text{Au}_1@15\text{-crown-5}$. The catalytic reaction was performed on p-nitrophenol. Briefly, fresh NaBH_4 aqueous solution (25 mL; 0.1 M) and p-nitrophenol solution (25 mL; 2×10^{-4} M) were added into the round bottom flask and stirred for 15 min. After 15 min of stirring, synthesized $\text{Au}_1@15\text{-crown-5}$ was added to the mixture and stirred for 30 min. The color of the solution changed from yellow-green to colorless after 30 min of mixing, confirming the reduction in the p-nitrophenol to p-aminophenol. The calculation of TOF is described in the supporting information.

4. Conclusions

15-crown-5 was used as a protective agent in this research for the synthesis monodisperse $\text{Au}_1@15\text{-crown-5}$ by reducing H_2AuCl_4 with ethanol. The prepared $\text{Au}_1@15\text{-crown-5}$ was well characterized with UV-Vis, XPS, and HAADF-STEM, providing conclusive evidence for the formation of $\text{Au}_1(0)$. Moreover, the reasonable structure of the catalyst was proposed and verified further with XAS results. The synthesized $\text{Au}_1@15\text{-crown-5}$ was successfully used for the catalytic reduction in 4-nitrophenol to 4-aminophenol, and the catalyst can also be generalized to other nitrophenol and nitroaniline compounds. The results of this study show that zero-valent monodisperse Au_1 can be prepared in the 15-crown-5 ether, which can successfully be used for the catalytic reduction in toxic nitroaromatic to less toxic amino aromatic.

Supplementary Materials: The following supporting information can be downloaded at: <https://www.mdpi.com/article/10.3390/catal13040776/s1>, Figure S1: Energy Dispersive X-ray analysis; Figure S2: Comparison of K space and Q space of $\text{Au}@15\text{-crown-5/SiO}_2$ and Au foil: (a) $\text{Au}@15\text{-crown-5/SiO}_2$; (b) Au foil; Figure S3: XPS- Cl_{2p} spectra of 0.5 wt% $\text{Au}_1@15\text{-crown-5}$ catalyst; Table S1: Curve fit Parameters for Au K-edge EXAFS for $\text{Au}@15\text{-crown-5/SiO}_2$ Standard; Table S2: Comparing catalytic activities to the 4-NP reduction by several catalysts; Figure S4: Reduction of 4-NP in 4 min; Figure S5: spherical aberration electron microscopic images of $\text{Au}@15\text{-crown-5}$ after the reaction: (a) Monodisperse catalyst after reaction. (b) Catalyst agglomerated after reaction. References [14,15,27–39] are cited in the supplementary materials.

Author Contributions: Conceptualization, K.L.; investigation, X.S.; methodology, X.S.; software, K.L.; data curation, X.S.; writing—original draft preparation, X.S.; writing—review and editing, X.S. and K.L.; and supervision, K.L. All authors have read and agreed to the published version of the manuscript.

Funding: This research received no external funding.

Data Availability Statement: The data that support the findings in the work are available from the corresponding author upon reasonable request.

Conflicts of Interest: The authors declare no conflict of interest.

References

1. Gorin, D.J.; Toste, F.D. Relativistic effects in homogeneous gold catalysis. *Nature* **2007**, *446*, 395–403. [[CrossRef](#)] [[PubMed](#)]
2. Fujita, T.; Guan, P.; McKenna, K.; Lang, X.; Hirata, A.; Zhang, L.; Chen, M. Atomic origins of the high catalytic activity of nanoporous gold. *Nat. Mater.* **2012**, *11*, 775–780. [[CrossRef](#)] [[PubMed](#)]
3. Hashmi, A.S.K. Gold-catalyzed organic reactions. *Chem. Rev.* **2007**, *107*, 3180–3211. [[CrossRef](#)] [[PubMed](#)]
4. Sennewald, K.; Vogt, W.; Erpenbach, H.; Glaser, H.; Dyrschka, H. Carrier Catalyst for the Manufacture of Unsaturated Esters of Carboxylic Acids. U.S. Patent 3,650,986, 21 March 1968.
5. Qiao, B.; Liang, J.-X.; Wang, A.; Liu, J.; Zhang, T. Single atom gold catalysts for low-temperature CO oxidation. *Chin. J. Catal.* **2016**, *37*, 1580–1587. [[CrossRef](#)]
6. Cisneros, L.; Serna, P.; Corma, A. Selective reductive coupling of nitro aliphatic compounds with aldehydes in hydrogen using gold catalyst. *Chin. J. Catal.* **2016**, *37*, 1756–1763. [[CrossRef](#)]
7. Dong, J.; Zhu, M.; Zhang, G.; Liu, Y.; Cao, Y.; Liu, S.; Wang, Y. Highly selective supported gold catalyst for CO-driven reduction of furfural in aqueous media. *Chin. J. Catal.* **2016**, *37*, 1669–1675. [[CrossRef](#)]
8. Qiao, B.; Wang, A.; Yang, X.; Allard, L.F.; Jiang, Z.; Cui, Y.; Liu, J.; Li, J.; Zhang, T. Single-atom catalysis of CO oxidation using Pt₁/FeO_x. *Nat. Chem.* **2011**, *3*, 634–641. [[CrossRef](#)]
9. Chen, F.; Jiang, X.; Zhang, L.; Lang, R.; Qiao, B. Single-atom catalysis: Bridging the homo- and heterogeneous catalysis. *Chin. J. Catal.* **2018**, *39*, 893–898. [[CrossRef](#)]
10. Zhang, A.; Zhou, M.; Liu, S.; Chai, M.; Jiang, S. Synthesis of single-atom catalysts through top-down atomization approaches. *Front. Chem.* **2021**, *1*, 754167. [[CrossRef](#)]
11. Liu, K.; Hou, G.; Mao, J.; Xu, Z.; Yan, P.; Li, H.; Guo, X.; Bai, S.; Zhang, Z.C. Genesis of electron deficient Pt₁(0) in PDMS-PEG aggregates. *Nat. Commun.* **2019**, *10*, 996. [[CrossRef](#)]
12. Liu, K.; Shen, X.; Bai, S.; Zhang, Z.C. Stable discrete Pt₁(0) in crown ether with ultra-high hydrosilylation activity. *ChemCatChem* **2020**, *12*, 267–272. [[CrossRef](#)]
13. Li, H.X.; Liang, C.H.; Liu, K.R.; Hou, G.J.; Bai, S.; Zhang, Z.C. Bi/trinuclear Pt_{1,2}Cu cluster assembly from isolated metal atoms. *Chem. Commun.* **2022**, *58*, 4176–4179. [[CrossRef](#)] [[PubMed](#)]
14. Chen, Y.; Feng, L.; Sadeghzadeh, S.M. Reduction of 4-nitrophenol and 2-nitroaniline using immobilized CoMn₂O₄ NPs on lignin supported on FPS. *RSC. Adv.* **2020**, *10*, 19553–19561. [[CrossRef](#)]
15. Alshammari, K.; Niu, Y.; Palmer, R.E.; Dimitratos, N. Optimization of sol-immobilized bimetallic Au-Pd/TiO₂ catalysts: Reduction of 4-nitrophenol to 4-aminophenol for wastewater remediation. *Philos. Trans. R. Soc. A* **2020**, *378*, 20200057. [[CrossRef](#)] [[PubMed](#)]
16. Din, M.I.; Khalid, R.; Hussain, Z.; Hussain, T.; Mujahid, A.; Najeeb, J.; Izhar, F. Nanocatalytic assemblies for catalytic reduction of nitrophenols: A critical review. *Crit. Rev. Anal. Chem.* **2020**, *50*, 322–338. [[CrossRef](#)]
17. Wang, Z.Z.; Zhai, S.R.; Zhai, B.; Xiao, Z.Y.; An, Q.D. Preparation and catalytic properties of nano-Au catalytic materials based on the reduction of 4-Nitrophenol. *Prog. Chem.* **2014**, *26*, 234–247.
18. Wen, F.; Wang, D.; Zhang, X.; Qiao, N.; Sun, Y.; Zhang, H. Electro-Fenton degradation of p-nitrophenol using Fe/chi-mwnts modified graphite cathode. *Technol. Water Treat.* **2014**, *40*, 62–65,69.
19. Osin, O.A.; Yu, T.; Cai, X.; Jiang, Y.; Peng, G.; Cheng, X.; Li, R.; Qin, Y.; Lin, S. Photocatalytic degradation of 4-Nitrophenol by C, N-TiO₂: Degradation efficiency vs. embryonic toxicity of the resulting compounds. *Front. Chem.* **2018**, *6*, 192. [[CrossRef](#)]
20. Chen, L.; Du, Y.; Wang, H.; Lu, J.; He, M. Electrochemical reduction of m-Nitrophenol. *Fine Chem.* **2003**, *20*, 673–675.
21. Zhao, P.; Feng, X.; Huang, D.; Yang, G.; Astruc, D. Basic concepts and recent advances in nitrophenol reduction by gold- and other transition metal nanoparticles. *Coord. Chem. Rev.* **2015**, *287*, 114–136. [[CrossRef](#)]
22. Dai, Y.; Yu, P.; Zhang, X.; Zhuo, R. Gold nanoparticles stabilized by amphiphilic hyperbranched polymers for catalytic reduction of 4-Nitrophenol. *J. Catal.* **2016**, *337*, 65–71. [[CrossRef](#)]
23. Shang, Y.; Min, C.; Hu, J.; Wang, T.; Liu, H.; Hu, Y. Synthesis of gold nanoparticles by reduction of HAuCl₄ under UV irradiation. *Solid State Sci.* **2013**, *15*, 17–23. [[CrossRef](#)]
24. Sakamoto, M.; Tachikawa, T.; Fujitsuka, M.; Majima, T. Acceleration of laser-induced formation of gold nanoparticles in a poly(vinyl alcohol) film. *Langmuir* **2006**, *22*, 6361–6366. [[CrossRef](#)]
25. Turner, N.H.; Single, A.M. Determination of peak positions and areas from wide-scan XPS spectra. *Surf. Interface Anal.* **1990**, *15*, 215–222. [[CrossRef](#)]

26. Li, Y.g.; Quan, X.; Hu, C.; Li, C. Effective Catalytic Reduction of 4-Nitrophenol to 4-Aminophenol over Etched Halloysite Nanotubes@ α -Ni(OH)₂. *ACS Appl. Energy Mater.* **2020**, *3*, 4756–4766. [[CrossRef](#)]
27. Wang, Z.; Lin, G.; Li, S.; Hao, W.; Yu, R. Facile one-pot synthesis of MOF supported gold pseudo-single-atom catalysts for hydrogenation reactions. *R. Soc. Chem.* **2018**, *2*, 1024–1030. [[CrossRef](#)]
28. Choi, Y.; Bae, H.S.; Seo, E.; Jang, S.; Kim, B.S. Hybrid gold nanoparticle-reduced graphene oxide nanosheets as active catalysts for highly efficient reduction of nitroarenes. *J. Mater. Chem.* **2011**, *21*, 15431–15436. [[CrossRef](#)]
29. Xi, J.; Sun, H.; Wang, D.; Zhang, Z.; Duan, X.; Xiao, J.; Xiao, F.; Liu, L.; Wang, S. Confined-interface-directed synthesis of Palladium single-atom catalysts on graphene/amorphous carbon. *Appl. Catal. B Environ.* **2018**, *225*, 291–297. [[CrossRef](#)]
30. Li, J.; Zhong, L.; Tong, L.; Yu, Y.; Zhang, J. Atomic Pd on graphdiyne/graphene heterostructure as efficient catalyst for aromatic nitroreduction. *Adv. Funct. Mater.* **2019**, *29*, 1905423. [[CrossRef](#)]
31. Qin, L.; Yi, H.; Zeng, G.; Lai, C.; Huang, D.; Xu, P.; Fu, Y.; He, J.; Li, B.; Zhang, C.; et al. Hierarchical porous carbon material restricted Au catalyst for highly catalytic reduction of nitroaromatics. *J. Hazard. Mater.* **2019**, *380*, 120864. [[CrossRef](#)]
32. Liu, L.; Chen, R.; Liu, W.; Wu, J.; Gao, D. Catalytic reduction of 4-nitrophenol over Ni-Pd nanodimers supported on nitrogen-doped reduced graphene oxide. *J. Hazard. Mater.* **2016**, *320*, 96–104. [[CrossRef](#)] [[PubMed](#)]
33. Cai, R.; Ellis, P.R.; Yin, J.; Liu, J.; Brown, C.M.; Griffin, R.; Chang, G.; Yang, D.; Ren, J.; Cooke, K. Performance of preformed Au/Cu nanoclusters deposited on MgO powders in the catalytic reduction of 4-Nitrophenol in solution. *Small* **2018**, *14*, 1703734. [[CrossRef](#)] [[PubMed](#)]
34. Fernandes, D.M.; Rocha, M.; Rivera-Cárcamo, C.; Serp, P.; Freire, C. Ru single atoms and nanoparticles on carbon nanotubes as multifunctional catalysts. *Dalton Trans.* **2020**, *49*, 10250–10260. [[CrossRef](#)]
35. Liang, J.; Song, Q.; Wu, J.; Lei, Q.; Lee, C.S. Anchoring Copper Single Atoms on Porous Boron Nitride Nanofiber to Boost Selective Reduction of Nitroaromatics. *ACS Nano* **2021**, *16*, 4152–4161. [[CrossRef](#)] [[PubMed](#)]
36. Tian, Z.; Deng, X.; He, P.; Wang, G. Atomic Pt anchored on hierarchically porous monolithic carbon nanowires as high-performance catalyst for liquid hydrogenation. *Nano Res.* **2022**, *1*–7. [[CrossRef](#)]
37. Du, Z.; Qin, J.; Zhang, K.; Jia, L.; Tian, K.; Zhang, J.; Xie, H. N-doped carbon nanosheets supported-single Fe atom for p-nitrophenol degradation via peroxymonosulfate activation. *Appl. Surf. Sci.* **2022**, *591*, 153124. [[CrossRef](#)]
38. Zhang, M.; Liu, Y.; Zhao, H.; Tao, J.; Zhai, Y. Pd Anchored on a phytic acid/thiourea polymer as a highly active and stable catalyst for the reduction of nitroarene. *ACS Appl. Mater. Interfaces* **2021**, *13*, 19904–19914. [[CrossRef](#)]
39. Muhammad, I.; Khan, M.I.; Bahadar, K.S.; Kalsoom, A.; Ali, K.M.; Asiri, A.M. Catalytic reduction of picric acid, nitrophenols and organic azo dyes via green synthesized plant supported Ag nanoparticles. *J. Mol. Liq.* **2018**, *268*, 87–101.

Disclaimer/Publisher's Note: The statements, opinions and data contained in all publications are solely those of the individual author(s) and contributor(s) and not of MDPI and/or the editor(s). MDPI and/or the editor(s) disclaim responsibility for any injury to people or property resulting from any ideas, methods, instructions or products referred to in the content.